Rare Earth Metal Alkyl Complexes with Methyl-Substituted Triazacyclononane−amide Ligands: Ligand Variation and Ethylene Polymerization Catalysis

ARTICLE *in* ORGANOMETALLICS · FEBRUARY 2007

Impact Factor: 4.13 · DOI: 10.1021/om060870a

5 AUTHORS, INCLUDING:

Auke Meetsma
University of Groningen
527 PUBLICATIONS **15,547** CITATIONS

SEE PROFILE

Rare Earth Metal Alkyl Complexes with Methyl-Substituted Triazacyclononane-amide Ligands: Ligand Variation and Ethylene Polymerization Catalysis

Sergio Bambirra, Daan van Leusen, Cornelis G. J. Tazelaar, Auke Meetsma, and Bart Hessen*

Center for Catalytic Olefin Polymerization, Stratingh Institute for Chemistry and Chemical Engineering, University of Groningen, Nijenborgh 4, 9747 AG Groningen, The Netherlands

Received September 22, 2006

A series of rare earth metal dialkyl complexes was prepared with the general formula [Me_2TACN-(B)-NR]M(CH_2SiMe_3)$_2$ (TACN = 1,4,7-triazacyclononane, B = $(CH_2)_2$, $SiMe_2$; R = *t*Bu, *sec*Bu, *n*Bu; M = Sc, Y, Nd, La). For M = Sc, mixed monoalkyl−monochloro complexes were also accessible. Selected examples of these complexes were structurally characterized and show the metal in a distorted octahedral environment. With Lewis or Brønsted acid activators the dialkyl compounds can be converted to the corresponding monoalkyl cations, which were characterized by NMR spectroscopy. Comparative testing in catalytic ethylene polymerization showed that the catalyst activity is most strongly influenced by the metal ionic radius, but that variations in the ligand backbone and substitution pattern do influence other factors, such as polymer molecular weight and catalyst stability. Catalysts with the intermediately sized rare earth metal yttrium generally showed the highest activity, but some of these catalysts produce polyethylene with broad molecular weight distributions, suggesting multisite behavior. Hypothetically this could be caused by intermolecular ligand scrambling processes. Evidence that these may occur was found in the isolation of the "half-flyover" bimetallic yttrium complex {[η^3:η^1-[Me_2TACN(CH_2)$_2$N*t*Bu]Y(CH_2SiMe_3)}{η^3:μ-η^1-[Me_2TACN(CH_2)$_2$N*t*Bu]Y(CH_2SiMe_3)$_3$.

Introduction

Cationic alkyl complexes of the rare earth metals (i.e., group 3 and lanthanide metals)[1] have only recently emerged as a family of active olefin polymerization catalysts alongside those of the much more established cationic transition-metal alkyl catalysts.[2] Over the last few years, the effect of metal ionic radius (a uniquely tunable parameter for the trivalent rare earth metal ions) on ethylene polymerization catalysis has been demonstrated,[3] and encouraging reports have appeared on the applicability of these catalysts to the polymerization of 1-alkenes.[4] Nevertheless, much still needs to be discovered with respect to the properties and possibilities of this family of catalysts. One of these aspects is the way in which catalyst performance responds to variations in the ligand system.

Earlier we reported on a tetradentate monoanionic ancillary ligand system for cationic rare earth metal alkyl catalysts incorporating the 1,4,7-triazacyclononane (TACN) *fac*-tridentate donor fragment and a pendent amide functionality.[5] This ligand type (**A**) is related to the well-known dianionic cyclopentadienyl-amide ligands (**B**) used for cationic group 4 metal alkyl catalysts for olefin (co-)polymerization,[6] and its framework allows for variations in several features. As we observed that the presence of *i*Pr substituents on the TACN amine nitrogens gives rise to decomposition reactions via intramolecular metalation of the *i*Pr methyl groups,[5d] we used the *N*,*N*′-dimethyl-TACN moiety as the basis of a systematic study. Here we describe variations in the pendent amide moiety (both in the bridge and the amide substituent) in the Me_2TACN-amide ligand system. Combined

* Corresponding author. E-mail: B.Hessen@rug.nl.

(1) For recent reviews on cationic organometallic complexes of the rare earth metals see: (a) Arndt, S.; Okuda, J. *Adv. Synth. Catal.* **2005**, *347*, 339. (b) Zeimentz, P. M.; Arndt, S.; Elvidge, B. R.; Okuda, J. *Chem. Rev.* **2006**, *106*, 2404. (c) Hou, Z.; Luo, Y.; Li, X. *J. Organomet. Chem.* **2006**, *691*, 3114.

(2) For reviews on transition-metal cationic olefin polymerization catalysts, see: (a) Bochmann, M. *J. Chem. Soc., Dalton Trans.* **1996**, 255. (b) Brintzinger, H. H.; Fischer, D.; Mülhaupt, R.; Rieger, B.; Waymouth, R. M.; *Angew. Chem., Int. Ed. Engl.* **1995**, *34*, 1143. (c) Guram, A. S.; Jordan, R. F In *Comprehensive Organometallic Chemistry II*; Lappert, M. F., Ed.; Elsevier Scientific Ltd: Oxford, 1995; Vol. 4, p 589. (d) McKnight, A. L.; Waymouth, R. M. *Chem. Rev.* **1998**, *98*, 2587. (e) Resconi, L.; Cavallo, L.; Fait, A.; Piemontesi, F. *Chem. Rev.* **2000**, *100*, 1253. (f) Gibson, V. C.; Spitzmesser, S. K. *Chem. Rev.* **2003**, *103*, 283. (g) Alt, H. G.; Köppl, A. *Chem. Rev.* **2000**, *100*, 1205. (h) Coates, G. W. *Chem. Rev.* **2000**, *100*, 1223.

(3) (a) Arndt, S.; Spaniol, T. P.; Okuda, J. *Angew. Chem., Int. Ed.* **2003**, *42*, 5075. (b) Bambirra, S., Bouwkamp, M. W.; Meetsma, A.; Hessen, B. *J. Am. Chem. Soc.* **2004**, *126*, 9182.

(4) Li, X.; Baldamus, J.; Hou, Z. *Angew. Chem., Int. Ed.* **2005**, *44*, 962. (b) Luo, Y.; Baldamus, J.; Hou, Z. *J. Am. Chem. Soc.* **2004**, *126*, 13910. (c) Zhang, L.; Luo, Y.; Hou, Z. *J. Am. Chem. Soc.* **2005**, *127*, 14562. (d) Li, X.; Hou, Z. *Macromolecules* **2005**, *38*, 6767. (e) Ward, B. D.; Bellemin-Laponnaz, S.; Gade, L. H. *Angew. Chem., Int. Ed.* **2005**, *44*, 1668.

(5) (a) Bambirra, S.; van Leusen, D.; Meetsma, A.; Hessen, B.; Teuben, J. H. *Chem. Commun.* **2001**, 637. (b) Hessen, B.; Bambirra, S. (ExxonMobil) World Pat. WO02/32909, 2002. (c) Tazelaar, C. G. J.; Bambirra, S.; Van, Leusen, D.; Meetsma, A.; Hessen, B.; Teuben, J. H. *Organometallics* **2004**, *23*, 936. (d) Bambirra, S.; Meetsma, A.; Hessen, B. Bruins, A. P. *Organometallics* **2006**, *25*, 3486.

(6) (a) Shapiro, P. J.; Bunel, E.; Schaefer, W. P.; Bercaw, J. E. *Organometallics* **1990**, *9*, 867. (b) Shapiro, P. J.; Cotter, W. D.; Schaefer, W. P.; Labinger, J. A.; Bercaw, J. E. *J. Am. Chem. Soc.* **1994**, *116*, 4623. (c) Piers, W. E.; Shapiro, P. J.; Bunel, E.; Bercaw, J. E. *Synlett* **1990**, *1*, 74. (d) Stevens, J. C.; Timmers, F. J.; Wilson, D. R.; Schmidt, G. F.; Nickias, P. N.; Rosen, R. K.; Knight, G. W.; Lai, S. Y. (Dow) EP0416815, 1991. (e) Canich, J. A. M.; (Exxon) PCT WO9104257, 1991. (f) Okuda, J.; Schattenmann, F. J.; Wocadlo, S.; Massa, W. *Organometallics* **1995**, *14*, 789−795. (g) Dias, H. V. R.; Wang, Z.; Bott, S. G. *J. Organomet. Chem.* **1996**, *508*, 91. (h) Xu, G. *Macromolecules* **1998**, *31*, 2395. (i) Alt, H. G.; Fottinger, K.; Milius, W. *J. Organomet. Chem.* **1999**, *572*, 21. (j) Razavi, A.; Thewalt, U. *J. Organomet. Chem.* **2001**, *621*, 267. (k) Lanza, G.; Fragala, I. L.; Marks, T. J. *Organometallics* **2002**, *21*, 5594.

10.1021/om060870a CCC: $37.00
Publication on Web 01/18/2007

Chart 1

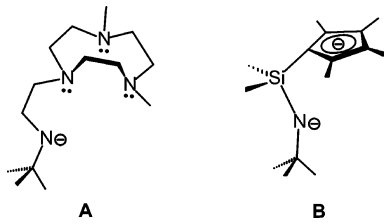

Scheme 1

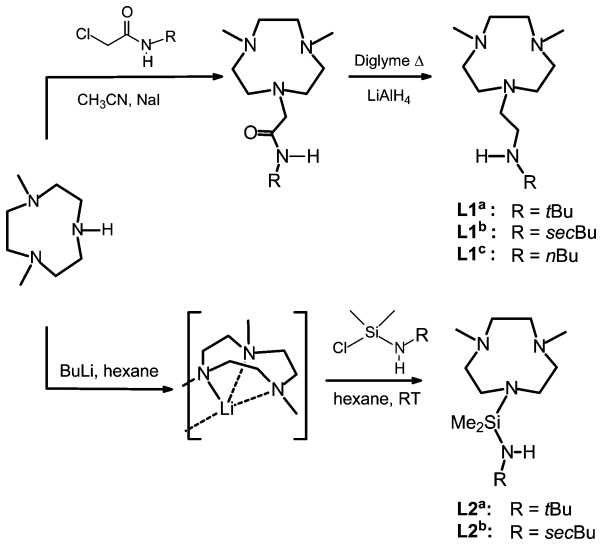

with variations in the ionic radius of the metal center and in the cocatalyst employed, this should serve as a probe to assess the effect of these variations on ethylene polymerization characteristics of cationic rare earth metal alkyl catalysts.

Results and Discussion

Ligand Synthesis. The ligands prepared in this study have the general formula $(Me_2TACN)-(bridge)-NHR$, with R = *t*Bu, *sec*Bu, or *n*Bu and with either $(CH_2)_2$ or $SiMe_2$ as the bridging moiety. The ligands with the $(CH_2)_2$ bridge were prepared by reaction of known 1,4-dimethyl-1,4,7-triazacyclononane[7] with various *N*-alkyl-α-chloro-acetamides, followed by reduction of the carbonyl function by reaction with $LiAlH_4$ and subsequent hydrolysis (Scheme 1), generally following the procedure recently detailed by us in the synthesis of related *i*Pr_2-TACN-amide ligands.[5d] The ligands are thermally and hydrolytically stable and can be purified by Kugelrohr distillation and/or acid−base extraction. *N*-Alkyl-2-(4,7-dimethyl-1,4,7-triazacyclononan-1-yl)ethylamine ligands $Me_2TACN(CH_2)_2$-NHR prepared in this way have R = *t*Bu (H**L1**[a]); *sec*Bu (H**L1**[b]); and *n*Bu (H**L1**[c]).

Ligands with the $SiMe_2$ bridge are most conveniently prepared by the lithiation of the appropriate 1,4-dialkyl-1,4,7-triazacyclononane with *n*-BuLi,[8] followed by reaction with the desired alkylamido(dimethyl)chlorosilane (Scheme 1). These ligands are sensitive to hydrolysis and were mostly used as the crude product (>95% pure by NMR spectroscopy) obtained by filtration of the reaction mixture followed by removal of the solvent in vacuum. *N*-Alkyl-2-(4,7-dimethyl-1,4,7-triazacyclononan-1-yl)dimethylsilylamine ligands $Me_2TACNSiMe_2NHR$ prepared in this way have substituents R = *t*Bu (H**L2**[a]) and *sec*Bu (H**L2**[b]).

Scheme 2

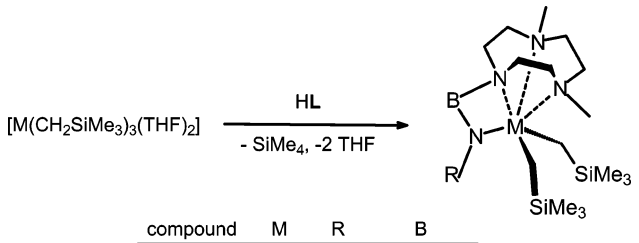

compound	M	R	B
1a	Sc	*t*Bu	Me_2Si
1b	Sc	*sec*Bu	Me_2Si
2a	Y	*t*Bu	$(CH_2)_2$
2b	Y	*sec*Bu	$(CH_2)_2$
2c	Y	*n*Bu	$(CH_2)_2$
3a	Y	*t*Bu	Me_2Si
3b	Y	*sec*Bu	Me_2Si

Scheme 3

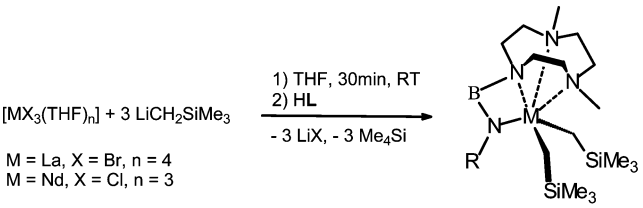

compound	M	R	B
4a	La	*t*Bu	$(CH_2)_2$
5a	Nd	*t*Bu	$(CH_2)_2$
5b	Nd	*sec*Bu	$(CH_2)_2$
6a	Nd	*t*Bu	Me_2Si
6b	Nd	*sec*Bu	Me_2Si

Synthesis of R_2TACN-Amide Metal Dialkyl Complexes. For the metals for which the homoleptic trialkyl complexes $M(CH_2SiMe_3)_3(THF)_2$ are available (M = Sc, Y, Sm−Lu)[9,3a] a convenient way to prepare the dialkyl complexes (**L**)$M(CH_2SiMe_3)_2$ is the reaction of the corresponding trialkyl with H**L** in pentane or THF solvent. For Sc and Y these reactions were seen to be quantitative on the NMR-tube scale and on a preparative scale afford the products **1**−**4** (Scheme 2) as crystalline solids after crystallization from pentane in 70−80% isolated yield. Interestingly, for the combination of **L1**[a] and Y in pentane a side reaction is observed (vide infra), which makes THF the solvent of choice to prepare **2a**.

For the larger lanthanide metals, the neutral homoleptic trialkyls $M(CH_2SiMe_3)_3(THF)_n$ are not available and thus cannot be employed as preformed starting materials. Nevertheless, it proved possible to obtain the TACN-amide dialkyl complexes of lanthanum and neodymium using an *in situ* alkylation procedure.[3b,5c] Reaction of $LaBr_3(THF)_4$ or $NdCl_3(THF)_3$ with 3 equiv of Me_3SiCH_2Li in THF (at ambient temperature) followed by addition of the appropriate H**L** species, evaporation

(7) Flassbeck, C.; Wieghardt, K. *Z. Anorg. Allg. Chem.* **1992**, *608*, 60.

(8) (a) Dubberley, S. R.; Mountford, P.; Adams, N. *Acta Crystallogr.* **2002**, *E58*, m342. (b) Fletcher, J. S.; Male, N. A. H.; Wilson, P. J.; Rees, L. H.; Mountford, P.; Schröder, M. *J. Chem. Soc., Dalton Trans.* **2000**, 4130.

(9) $M(CH_2SiMe_3)_3(THF)_n$: (a) Lappert, M. F.; Pearce, R. *J. Chem. Soc., Chem. Commun.* **1973**, 126. (b) Schumann, H.; Müller, J. *J. Organomet. Chem.* **1978**, *146*, C5. (c) Schumann, H.; Müller, J. *J. Organomet. Chem.* **1979**, *169*, C1. (d) Atwood, J. L.; Hunter, W. E.; Rogers, R. D. Holton, J.; McMeeking, J.; Pearce, R.; Lappert, M. F. *J. Chem. Soc., Chem. Commun.* **1978**, 140. (e) Niemeyer, M. *Acta Crystallogr.* **2001**, *E57*, m553. (f) Evans, W. J.; Brady, J. C.; Ziller, J. W. *J. Am. Chem. Soc.* **2001**, *123*, 7711. (g) Arndt, S.; Spaniol, T. P.; Okuda, *Chem. Commun.* **2002**, 896. (h) Qi, G.; Nitto, Y.; Saiki, A.; Tomohiro, T.; Nakayama, Y.; Yasuda, H. *Tetrahedron* **2003**, *59*, 10409.

Scheme 4

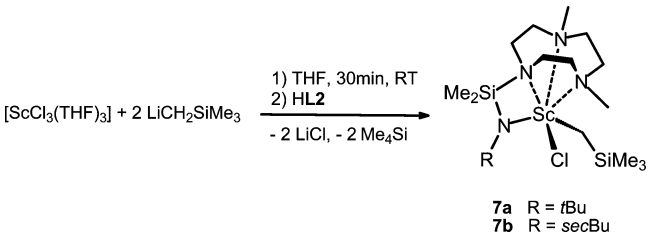

7a R = *t*Bu
7b R = *sec*Bu

Scheme 5

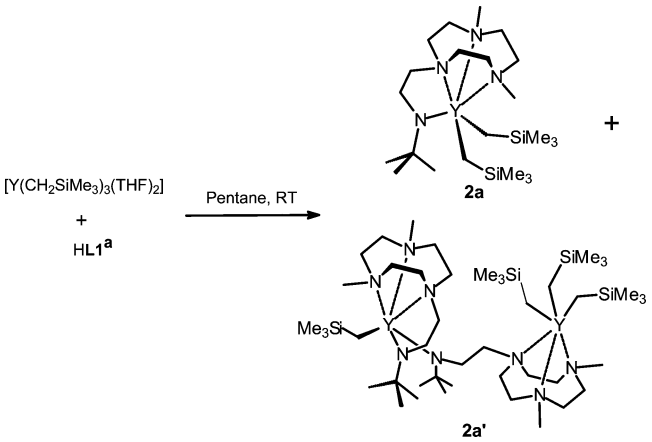

of the volatiles, and extraction with pentane (Scheme 3) resulted in isolation of the desired compounds in moderate yield (around 50%).

This *in situ* alkylation procedure also allowed the synthesis of scandium monoalkyl−monochloride complexes **7a** and **7b**, by initial reaction of $ScCl_3(THF)_3$ with 2 equiv of Me_3SiCH_2-Li, followed by addition of the TACN-amine (Scheme 4). Apparently the TACN-amide ligand provides sufficient protection of the metal center to prevent formation of LiCl adducts or ate-complexes, making this method very versatile.

All TACN-amide dialkyl compounds reported here are highly air-sensitive, but thermally stable in solution at ambient temperature for at least 1 day. To this, there is one notable exception: attempts to prepare the dialkyl compound with the largest metal (La) and the $SiMe_2$-bridged ligand **L2**[a] resulted only in isolation of the dinuclear complex $\{[(\mu\text{-}CH_2)MeTACN(SiMe_2)NtBu]La(CH_2SiMe_3)\}_2$, which stems from (intermolecular) metalation of the TACN methyl substituent. Preparation and structural characterization of **8** were communicated before[5c] and will not be detailed here.

Another potential complication was spotted when the reaction between $Y(CH_2SiMe_3)_3(THF)_2$ and H**L1**[a] was performed in *pentane* solvent. In addition to the expected product **2a**, formation of an appreciable amount of the poorly soluble dinuclear complex $\{[\eta^3{:}\eta^1\text{-}[Me_2TACN(CH_2)_2NtBu]Y(CH_2SiMe_3)\}\{\eta^3{:}\mu\text{-}\eta^1\text{-}[Me_2TACN(CH_2)_2NtBu]Y(CH_2SiMe_3)_3$ (**2a′**) was observed (Scheme 5). One of the two TACN-amide ligands in this compound (which was structurally characterized, vide infra) is bound to one metal with its triamine moiety, while the amide group is bound to the other metal. Formation of this product was not observed when the reaction was performed in THF solvent. Isolated **2a** did not rearrange to give **2a′** in any solvent, suggesting that the latter is a kinetic product when the synthesis is performed in pentane. None of the other ligand−metal combinations gave rise to products related to **2a′**.

Structure Determinations. Single-crystal X-ray structure determinations were performed on the dialkyl complexes [Me_2-

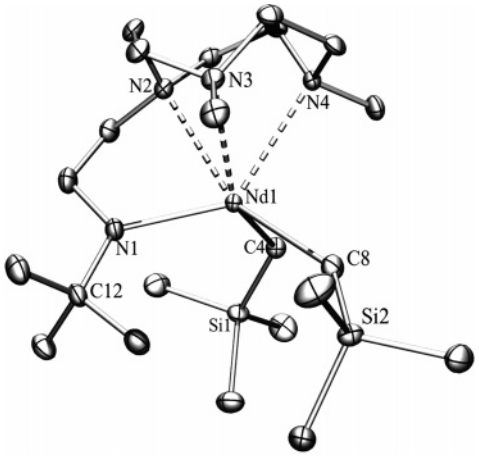

Figure 1. Molecular structure of $[Me_2TACN(CH_2)_2NtBu]Nd(CH_2SiMe_3)_2$ (**5a**) (ellipsoid probability level at 50%).

Table 1. Selected Bond Lengths (Å) and Angles (deg) for 4a and 5a

	4a (M = La)	**5a** (M = Nd)
	Bond Lengths (Å)	
M−C(4)	2.618(2)	2.5566(19)
M−C(8)	2.632(2)	2.5688(19)
M−N(1)	2.3483(19)	2.2919(16)
M−N(2)	2.7202(19)	2.6607(15)
M−N(3)	2.7833(19)	2.7242(15)
M−N(4)	2.754(2)	2.7040(14)
	Bond Angles (deg)	
N(2)−M−N(1)	68.60(7)	69.94(5)
N(2)−M−C(8)	127.12(8)	126.81(6)
N(2)−M−C(4)	104.68(7)	104.29(6)
M−N(1)−C(12)	124.34(14)	124.69(11)

$TACN(CH_2)_2NtBu]M(CH_2SiMe_3)_2$ (M = La **4a**, Nd **5a**) and $[Me_2TACN(SiMe_2)NR]M(CH_2SiMe_3)_2$ (M = Y, R = *t*Bu: **3a**, *sec*Bu: **3b**; M = Nd, R = *t*Bu: **6a**). The structure determinations of the Me_2TACN-amide dialkyl complexes with the $SiMe_2$ bridge were complicated by the occurrence of a low-temperature phase transition in the solids, causing splitting of the diffraction peaks. This is a feature that appeared to be common of all dialkyl derivatives with this bridging moiety described here, irrespective of the metal ion or amide substituent. To avoid this problem, structure determinations of these compounds were performed at relatively high temperature (230 K), resulting in successful structural characterization, but at lower accuracy due to increased thermal motion of the atoms.

All complexes show essentially a distorted octahedral geometry around the metal center. The general features of the complexes are similar to those reported previously for *i*Pr_2-TACN−B−N*t*Bu (B = $(CH_2)_2$, $SiMe_2$) Y and La dialkyls[5d] and will not be discussed in detail here.

The structures of [**L1**[a]]$M(CH_2SiMe_3)_2$ (M = Nd, **4a**; La, **5a**) are isomorphous. The molecular structure of the Nd derivative **5a** is shown in Figure 1, and Table 1 presents the geometrical data of **4a** and **5a** (that have identical atom labeling). Comparing the M−N and M−C distances for the Nd and La analogues shows that those for Nd are 0.05−0.06 Å shorter, corresponding to the difference in ionic radius for Nd^{3+} (0.98 Å) versus La^{3+} (1.03 Å).[10]

As can be seen from the comparison of the two Nd complexes **5a** and **6a**, (Figures 1 and 2; Tables 1 and 2, respectively), the Me_2Si bridge results in a smaller N(bridgehead)−M−N(amide)

(10) Effective ionic radius of Ln^{3+} for coordination number 6: Shannon, R. D. *Acta Crystallogr. Sect. A* **1976**, *32*, 751.

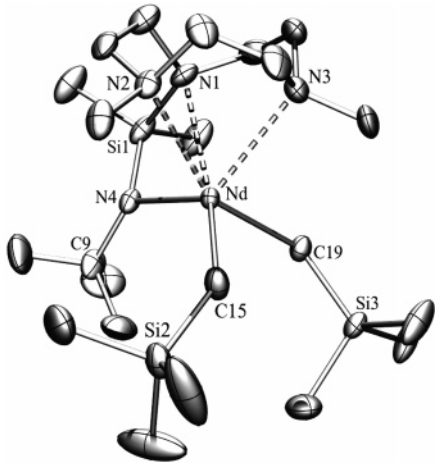

Figure 2. Molecular structure of [Me_2TACN($SiMe_2$)N*t*Bu]Nd(CH_2-$SiMe_3$)$_2$ (**6a**) (ellipsoid probability level at 30%).

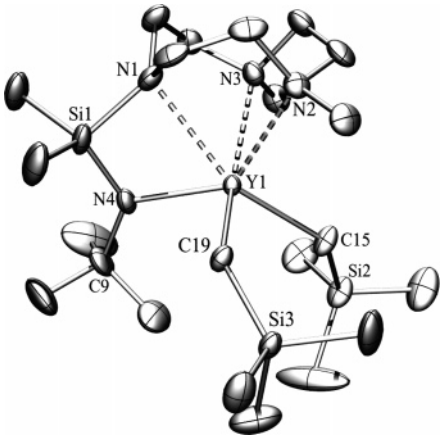

Figure 3. Molecular structure of [Me_2TACN($SiMe_2$)N*t*Bu]Y(CH_2-$SiMe_3$)$_2$ (**3a**) (ellipsoid probability level at 30%).

Table 2. Selected Bond Lengths (Å) and Angles (deg) for 3a, 3b, and 6a

	3a (M = Y)	**3b** (M = Y)	**6a** (M = Nd)
	Bond Lengths (Å)		
M−C(19)	2.462(3)	2.477(8)	2.567(6)
M−C(15)	2.436(4)	2.471(10)	2.533(8)
M−N(4)	2.248(3)	2.216(8)	2.320(6)
M−N(1)	2.602(3)	2.619(7)	2.753(6)
M−N(2)	2.549(3)	2.639(8)	2.771(6)
M−N(3)	2.654(3)	2.534(9)	2.664(6)
	Bond Angles (deg)		
N(1)−M−N(4)	65.29(12)	65.3(3)	62.56(19)
N(4)−M−C(15)	124.20(13)	108.0(3)	126.5(2)
N(4)−M−C(19)	95.16(12)	95.7(3)	94.38(19)
M−N(4)−C(9)	126.6(3)	130.7(7)	123.7(4)

bite angle and a reduced M−N(bridgehead) distance when compared to the $(CH_2)_2$-bridged analogue. The asymmetry of the complexes, especially visible in the difference between the two N(amide)−M−CH_2 angles, is associated with the twist in the ligand bridging moiety. The largest N(amide)−M−C angle is found for the alkyl group on the side to which the substituent on the amide is pointing. A decrease in size of the amide substituent from *t*Bu to *sec*Bu leads to a reduction of this angle, as can be seen in the Y complexes **3a** and **3b** (124.3° vs 108.0°, Table 2, Figures 3 and 4). The difference between *i*Pr and Me as substituents on the TACN amine groups can be seen by comparing the structure of compound **3a** with its *i*Pr$_2$TACN analogue.[5d] In the latter, the Y−N(amine) distance of the amine

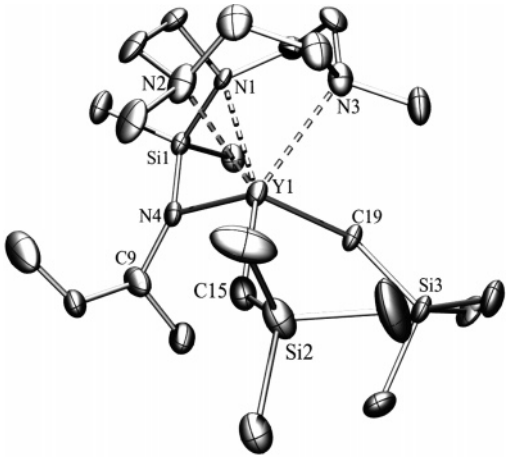

Figure 4. Molecular structure of [Me_2TACN($SiMe_2$)N*sec*Bu]Y(CH_2-$SiMe_3$)$_2$ (**3b**) (ellipsoid probability level at 30%).

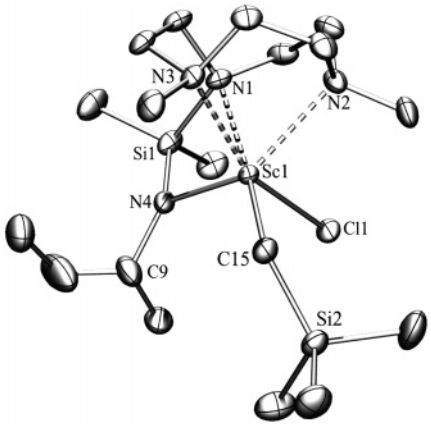

Figure 5. Molecular structure of {[Me_2TACN($SiMe_2$)N*sec*Bu]Sc-(CH_2SiMe_3)Cl} (**7b**) (ellipsoid probability level at 30%).

Table 3. Selected Bond Lengths (Å) and Angles (deg) for 7b

Bond Lengths (Å)		Bond Angles (deg)	
Sc(1)−C(15)	2.272(3)	N(1)−Sc(1)−C(15)	163.31(9)
Sc(1)−Cl(1)	2.4602(9)	N(3)−Sc(1)−Cl(1)	159.25(6)
Sc(1)−N(1)	2.399(2)	N(4)−Sc(1)−Cl(1)	95.57(6)
Sc(1)−N(2)	2.397(2)	N(4)−Sc(1)−C(15)	112.80(11)
Sc(1)−N(3)	2.442(2)	N(1)−Sc(1)−N(4)	70.56(8)
Sc(1)−N(4)	2.065(2)	Sc(1)−N(4)−C(9)	126.6(2)

group closest to one of the alkyl groups is substantially larger (by 0.1 Å), suggesting steric interference.

The structure of the scandium monoalkyl−monochloro complex **7b** is shown in Figure 4 (geometrical data in Table 3). The compound is monomeric, indicating that the ligand imparts sufficient protection to prevent the chloride from taking up a bridging position between two metal centers. The relatively small Sc metal center results in a larger N(bridgehead)−M−N(amide) bite angle (70.56(8)°) than those in the other complexes. The terminal Sc−Cl distance of 2.4604(9) Å is relatively long compared to other known examples.[11,12]

(11) ScClR: (a) Hayes, P. G.; Piers, W. E.; Lee, L. W. M.; Knight, L. K.; Parvez, M.; Elsegood, M. R. J.; Clegg, W. *Organometallics* **2001**, *20*, 2533. (b) Hayes, P. G Ph.D. Thesis, 2004, Calgary.

(12) Sc−Cl distances: (a) PNPScCl$_2$ Sc−Cl = 2.448; 2.418 Å: Fryzuk, M. D.; Giesbrecht, G.; Rettig, S. J. *Organometallics* **1996**, *15*, 3329. (b) LScCl2 Sc−Cl = 2.380; 2.356 Å: Lee, L. W. M.; Piers, W. E.; Elsegood, M. R. J.; Clegg, W.; Parvez, M. *Organometallics* **1999**, *18*, 2947. (c) Sc−Cl = 2.4426 and 2.3982 Å: Ward, B. D.; Dubberley, S. R.; Maisse-François, A.; Gade, L. H.; Mountford, P. *Dalton Trans*. **2002**, 4649. (d) Six-coordinate: Boyd, C. L.; Toupance, T.; Tyrrell, B. R.; Ward, B. D.; Wilson, C. R.; Cowley, A. R.; Moutford, P. *Organometallics* **2005**, *24*, 309.

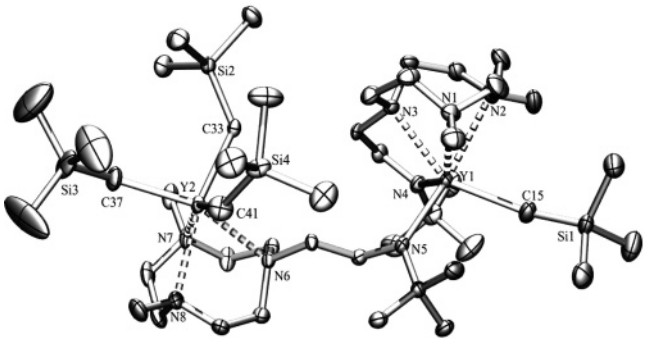

Figure 6. Molecular structure of **2a′** (ellipsoid probability level at 50%).

Table 4. Selected Bond Lengths (Å) and Angles (deg) for 2a′

	Bond Lengths (Å)		
Y(1)−C(15)	2.444(5)	Y(2)−C(33)	2.434(4)
Y(1)−N(1)	2.638(4)	Y(2)−C(37)	2.439(4)
Y(1)−N(2)	2.761(4)	Y(2)−C(41)	2.430(5)
Y(1)−N(3)	2.541(3)	Y(2)−N(6)	2.617(3)
Y(1)−N(4)	2.265(3)	Y(2)−N(7)	2.606(3)
Y(1)−N(5)	2.296(3)	Y(2)−N(8)	2.592(3)
	Bond Angles (deg)		
N(4)−Y(1)−C(15)	112.63(15)	N(4)−Y(1)−N(5)	97.95(11)
N(2)−Y(1)−N(5)	168.98(11)		

The dinuclear species **2a′** was also structurally characterized (Figure 6, geometrical data in Table 4). It may be considered as a "half-flyover" complex, in which one of the TACN-amide ligands is bridging the two metal centers. The TACN moiety of the ligand is *fac* trihapto bound to Y(2), which also bears three alkyl groups. This fragment is structurally similar to the known, structurally characterized, trialkyl $[Me_3TACN]Y(CH_2SiMe_3)_3$.[13] The pendent amide is bound to Y(1), which bears one tetrahapto TACN-amide ligand and one alkyl group. This metal center is the more sterically congested one, exemplified by the elongation of one of the Y−amine distances: Y(1)−N(2) = 2.761(4) Å.

NMR Spectroscopic Data. The diamagnetic (Y, La) dialkyl species with the $(CH_2)_2$ bridge and *t*Bu or *n*Bu amide substituents show low-temperature solution NMR spectra consistent with an asymmetric structure (corresponding to the solid-state structures), whereas at higher temperatures broadening and coalescence of resonances leads to spectra consistent with an averaged C_s symmetric structure. This behavior is the same as that recently described by us for iPr$_2$TACN-amide Y and La complexes.[5d] Unlike the iPr$_2$TACN-amide derivatives, the Me$_2$TACN-amide compounds with the $SiMe_2$ bridge did not reach the slow-exchange limit for this process down to −60 °C, indicating that the substituents on the TACN amine nitrogens do influence the conformation dynamics of these complexes. The compounds with the *sec*Bu amide substituent show asymmetric spectra at ambient temperature due to the asymmetry of the substituent, but only for the $(CH_2)_2$ bridge (**2b**) can two conformational diastereomers (in approximately 1:1 ratio) be observed at low temperature. From the coalescence behavior of the alkyl $SiMe_3$ protons, the barrier of symmetrization could be estimated[14] for the Y complexes with the $(CH_2)_2$ bridge **2a** ($\Delta G^{\ddagger}$ = 14.7(3) kcal/mol at 18.5 °C) and **2c** ($\Delta G^{\ddagger}$ = 12.3(3) kcal/mol at −18.9 °C). It is seen that upon changing the amide substituent from *t*Bu to *n*Bu, the latter complex shows more mobility due to the reduced steric interaction. Similarly, replacing the Y center in **2a** by the larger La (**4a**) causes a significant decrease in the symmetrization barrier ($\Delta G^{\ddagger}$ = 10.9-(3) kcal/mol at −57.1 °C).

The dinuclear yttrium complex **2b′** shows solution NMR spectra consistent with an asymmetric structure. Four separate alkyl $SiMe_3$ resonances can be seen, and (apart from one overlapping set) the alkyl methylene protons can be seen as separate ABX patterns.

Generation of Cationic Alkyl Species [LMR]$^+$. Upon reaction of the Me$_2$TACN-amide metal dialkyl complexes with $[PhNMe_2H][B(C_6F_5)_4]$ in the weakly coordinating polar solvent C_6D_5Br, the corresponding cationic monoalkyl species are generated cleanly (as seen by NMR spectroscopy) under liberation of $SiMe_4$ and free $PhNMe_2$. These cationic species are sufficiently stable to allow characterization by ^{1}H NMR spectroscopy at ambient temperature (although for ^{13}C NMR spectra the samples were sometimes cooled to −30 °C). This is in contrast to the cationic alkyl species with the iPr$_2$TACN-amide ligand, which, in the absence of coordinating solvents like THF, decomposed rapidly by intramolecular metalation of the ligand *i*Pr substituents.[5d] The cationic species show the typical downfield shift of the M−CH_2Si carbon resonances relative to the neutral parent dialkyls, and the Y derivatives show an increase in the $^1J_{YC}$ coupling constant.[3,5,15] The cationic La alkyl species $[(\mathbf{L1^a})La(CH_2SiMe_3)]^+$ shows a very broad ^{1}H $LaCH_2$ resonance at ambient temperature, and cooling the sample to −30 °C leads to a splitting into two diastereotopic protons (δ −0.23 and −0.89 ppm, $^2J_{HH}$ = 10.2 Hz). This is not observed for the Sc and Y cations and could indicate that the large ionic radius of La may allow the coordination of the aromatic solvent. The η^6-coordination of aromatics to cationic (β-diketiminate)Sc species was demonstrated previously by Piers et al.[16] Such an interaction with the aromatic solvent may account for the anomalous behavior of the La system in catalytic ethylene polymerization (vide infra). In this case it is unlikely that the *N*,*N*-dimethylaniline is involved, as its chemical shifts are fully consistent with the free aniline in bromobenzene solution.

Catalytic Ethylene Polymerization. Ethylene polymerization experiments were conducted with the series of complexes $[\mathbf{L}M(CH_2SiMe_3)_2]$ (M = Sc, Y, La and Nd) as precatalysts. These were activated by reaction with either $[PhNMe_2H][B(C_6F_5)_4]$ or $[Ph_3C][B(C_6F_5)_4]$ in toluene solvent under 5 bar of ethylene pressure, without additional use of alkylaluminum impurity scavengers. Runs were performed at 50 and 80 °C with a run time of 10 min.

In Table 5 the results are shown for the systems with the Me$_2$TACN−$SiMe_2$−N*t*Bu ligand. This allows a comparison between the metals Sc, Y, and Nd. For Sc a modest activity is found, which increases with increasing temperature. The trityl cation appears to be somewhat more effective as activator. The polydispersity of the PE indicates single-site behavior of the catalyst under all conditions. The polymer molecular weight is high at 50 °C (>6 × 10^5), but drops considerably upon increasing the temperature. The Y catalyst is considerably more

(13) (a) Tredget, C. S.; Lawrence, S. C.; Ward, B. D.; Howe, R. G.; Cowley, A. R.; Mountford, P. *Organometallics* **2005**, *24*, 3136. (b) Bambirra, S.; Meetsma, A.; Hessen, B. *Acta Crystallogr.* **2006**, *E62*, 314.

(14) Hesse, M.; Meier, H.; Zeeh, B. *Spekroskopische Methoden in der Organischen Chemie*; Georg Thieme Verlag: Stuttgart, New York, 1995.

(15) For other examples of these trends in rare earth metal alkyl species see: (a) Lee, L.; Berg, D. J.; Einstein, F. W.; Batchelor, R. J. *Organometallics* **1997**, *16*, 1819. (b) Reference 12b. (c) Elvidge, B. R.; Arndt, S.; Zeimentz, P. M.; Spaniol, T. P.; Okuda, J. *Inorg. Chem.* **2005**, *44*, 6777. (d) Cameron, T. M.; Gordon, J. C.; Michalczyk, R. Scott, B. L. *Chem. Commun.* **2003**, 2282.

(16) Hayes, P. G.; Piers, W. E.; Parvez, M. *J. Am. Chem. Soc.* **2003**, *125*, 5622.

Table 5. Ethylene Polymerization with [Me$_2$TACN(SiMe$_2$)N*t*Bu]M(CH$_2$SiMe$_3$)$_2$ (M = Sc, Y, Nd)[a]

M	activator	*T* (°C)	PE yield (g)	activity (kg/mol·h·bar)	M_w ($\times 10^{-3}$)	M_w/M_n
Sc	A	50	0.60	75	690	2.2
Sc	A	80	3.01	376	128	1.9
Sc	T	50	1.16	145	939	1.7
Sc	T	80	4.33	541	138	2.1
Y	A	50	10.75	1343	127	6.6
Y	A	80	9.06	1132	72	6.2
Y	T	50	10.24	1280	139	10.5
Y	T	80	13.62	1571	60	5.1
Nd	A	50	5.95	743	358	2.4
Nd	A	80	1.95	243	65	2.2
Nd	T	50	6.31	788	503	2.1
Nd	T	80	2.60	325	71	1.7

[a] 200 mL of toluene, 10 μmol of catalyst, 10 μmol of activator [PhNMe$_2$H][B(C$_6$F$_5$)$_4$] (A) or [Ph$_3$C][B(C$_6$F$_5$)$_4$] (T), 10 min run time.

Table 6. Ethylene Polymerization with [Me$_2$TACN(SiMe$_2$)N*sec*Bu]M(CH$_2$SiMe$_3$)$_2$ (M = Sc, Y, Nd)[a]

M	activator	*T* (°C)	PE yield (g)	activity (kg/mol·h·bar)	M_w ($\times 10^{-3}$)	M_w/M_n
Sc	A	50	1.63	203	350	1.4
Sc	A	80	1.96	245	157	3.5
Sc	T	50	2.72	340	484	1.8
Sc	T	80	2.90	362	135	2.7
Y	A	50	5.22	652	778	2.0
Y	A	80	8.45	1067	91	3.6
Y	T	50	10.23	1278	547	1.6
Y	T	80	15.54	1942	53	2.6
Nd	A	50	2.30	287	391	1.8
Nd	A	80	1.50	187	61	2.0
Nd	T	50	1.16	145	293	2.0
Nd	T	80	n.d.			

[a] 200 mL of toluene, 10 μmol of catalyst, 10 μmol of activator [PhNMe$_2$H][B(C$_6$F$_5$)$_4$] (A) or [Ph$_3$C][B(C$_6$F$_5$)$_4$] (T), 10 min run time.

Table 7. Ethylene Polymerization with [Me$_2$TACN(CH$_2$)$_2$N*t*Bu]M(CH$_2$SiMe$_3$)$_2$ (M = Y, Nd, La)[a]

M	activator	*T* (°C)	PE yield (g)	activity (kg/mol·h·bar)	M_w ($\times 10^{-3}$)	M_w/M_n
Y	A	50	9.40	1175	325	4.9
Y	A	80	14.30	1787	98	6.0
Y	T	50	14.49	1811	130	7.2
Y	T	80	17.60	2200	72	3.8
Nd	A	50	6.46	807	56	2.2
Nd	A	80	5.00	625	35	1.8
Nd	T	50	9.87	1233	69	2.3
Nd	T	80	3.86	482	38	1.9
La	A	50	0	0		
La	A	80	0	0		
La	T	50	0	0		
La	T	80	0	0		

[a] 200 mL of toluene, 10 μmol of catalyst, 10 μmol of activator [PhNMe$_2$H][B(C$_6$F$_5$)$_4$] (A) or [Ph$_3$C][B(C$_6$F$_5$)$_4$] (T), 10 min run time.

Table 8. Ethylene Polymerization with [Me$_2$TACN(CH$_2$)$_2$NR]Y(CH$_2$SiMe$_3$)$_2$ (R = *t*Bu, *sec*Bu, *n*Bu)[a]

R	activator	*T* (°C)	PE yield (g)	activity (kg/mol·h·bar)	M_w ($\times 10^{-3}$)	M_w/M_n
*t*Bu	A	50	9.40	1175	325	4.9
*t*Bu	A	80	14.30	1787	98	6.0
*t*Bu	T	50	14.49	1811	130	7.2
*t*Bu	T	80	17.60	2200	72	3.8
*sec*Bu	A	50	10.65	1331	90	3.8
*sec*Bu	A	80	16.13	2016	54	2.3
*sec*Bu	T	50	10.43	1303	135	4.3
*sec*Bu	T	80	16.22	2027	77	3.4
*n*Bu	A	50	2.28	285	294	2.6
*n*Bu	A	80	3.91	488	92	1.8
*n*Bu	T	50	5.11	638	703	2.4
*n*Bu	T	80	9.29	1157	151	3.1

[a] 200 mL of toluene, 10 μmol of catalyst, 10 μmol of activator [PhNMe$_2$H][B(C$_6$F$_5$)$_4$] (A) or [Ph$_3$C][B(C$_6$F$_5$)$_4$] (T), 10 min run time.

active (up to 1500 kg mol^{-1} h^{-1} bar^{-1}), but produces PE with a broad polydispersity (M_w/M_n = 5−10), suggesting the presence of multiple active species. This appears to be a general feature of the Y catalysts with Me$_2$TACN-amide ligands with the *t*Bu amide substituent (vide infra). Molecular weights are overall significantly lower than for Sc. The Nd catalyst shows intermediate activity (around 750 kg mol^{-1} h^{-1} bar^{-1} at 50 °C), but deactivates within a few minutes at 80 °C. Nevertheless, single-site behavior is observed under all conditions.

In Table 6 the data are given for the SiMe$_2$-bridged ligand system, but now with the *sec*Bu substituent (instead of *t*Bu) on the amide. For Sc this yields a catalyst with double the activity of the N*t*Bu analogue at 50 °C, but with a significantly decreased thermal stability, and producing PE with a lower M_w. For Y, the catalyst is highly active (up to 2000 kg mol^{-1} h^{-1} bar^{-1}) and now appears to show essentially single-site behavior, with polydispersities around 2.5. For Nd, the activity is clearly lower than for the N*t*Bu analogue, apparently due to a further decrease in thermal stability of the catalyst.

In Table 7, data are given for systems with the Me$_2$TACN−(CH$_2$)$_2$−N*t*Bu ligand, which can be directly compared to data in Table 5 of the analogues with the SiMe$_2$ bridge. For Y this appears to give a catalyst with improved activity at higher temperature, but again the polydispersity of the PE formed is relatively high (4−7). For the larger metal Nd, this (more sterically demanding) ligand gives the best activity, especially with a trityl cation as activator (>1200 kg mol^{-1} h^{-1} bar^{-1}), but the stability at elevated temperature is still poor. Interestingly, the polymer M_w for the Nd catalyst with the (CH$_2$)$_2$ bridge is substantially lower (by about a factor of 7) than that for the SiMe$_2$-bridged catalyst. Remarkably, the analogous La system is completely inactive for catalytic ethylene polymerization under the present conditions.

In Table 8, a series of data is given for the Y catalysts with the Me$_2$TACN−(CH$_2$)$_2$−NR (R = *t*Bu, *sec*Bu, *n*Bu) ligands. It can be seen that for R = *n*Bu the overall activity is lower, but that the PE produced has the narrowest polydispersity. It is also remarkable that for this (the sterically least encumbered) system the activity with the trityl borate activator is significantly higher than with the anilinium borate activator. This may suggest that here the liberated *N*,*N*-dimethylanilin can compete with ethylene for binding to the cationic metal center.

With the TACN-amide ancillary ligand system, the most active catalysts appear to be those with metals in the intermediate size range (in casu yttrium). A similar observation was made in the family of cationic monoamidinate rare earth metal alkyl catalysts.[3b] Although in that system the activity of the La derivative was low (14 kg mol^{-1} h^{-1} bar^{-1} at 30 °C), the complete lack of activity of the TACN-amide La catalyst is rather surprising. This could be associated with binding of toluene solvent to the large Lewis acidic metal center. An indication for metal−solvent interaction of the cationic La−CH$_2$SiMe$_3$ species with bromobenzene was obtained by low-temperature NMR spectroscopy (vide supra).

Although all polymerization experiments were run in the absence of alkylaluminum species, none of the TACN-amide catalysts showed living ethylene polymerization behavior. This is in marked contrast with our observations in the cationic amidinate yttrium alkyl catalyst system, which at 50 °C produced high molecular weight PE with very narrow (1.1−1.2) poly-

Table 9. Ethylene Polymerization of 2a′ in Comparison to 8[a]

catalyst	temp (°C)	PE (g)	productivity (kg mol^{-1} bar^{-1} h^{-1})	$10^3 M_w$	M_w/M_n
2a′ / A	50	6.0	752	495	2.42
2a′/ 2A	50	9.9	1240	276	7.66
8/A	50	3.8	481	1596	2.00
8/2 A	50	7.3	915	1244	2.02

[a] 200 mL of toluene, 10 μmol of catalyst (**2a′**, **8**), 10 μmol of $[PhNMe_2H][B(C_6F_5)_4]$ (A) activator, 10 min run time.

dispersities.[17] This indicates that β-H elimination processes in the TACN-amide rare earth metal catalysts are substantially more facile than in the (more electron-poor) catalysts with the amidinate ancillary ligand.

With respect to catalyst activity, variations in parts of the TACN-amide ligand seem to have less of an effect than variations in metal ionic radius. The strongest effect of the ligand bridging moiety was seen for Nd, where the less constrained $(CH_2)_2$ bridge led to a significantly improved activity, but accompanied by a substantial drop in polymer molecular weight. The most pronounced effect of the size of the amide substituent was seen in the yttrium system, where the small *n*Bu substituent caused a large differentiation in performance for the two activators, possibly by allowing the aniline coproduct of the anilinium borate activator to bind reversibly to the active center.

A typical feature of the yttrium TACN-amide catalysts is that the derivatives with the *t*Bu-amide group (dialkyls **2a** and **3a**) produce polymers with a broad molecular weight distribution that suggests multisite behavior. Although as yet we do not have conclusive evidence for one specific source of this effect, a hypothesis could be that ligand redistribution between metal centers is involved. We observed such a process during the synthesis of compound **2a** in noncoordinating solvents, where concomitantly the dinuclear complex **2a′** was formed (vide supra). In Table 9, ethylene polymerization experiments using **2a′** as catalyst precursor are described (using $[PhNMe_2H][B(C_6F_5)_4]$ activator at 50 °C), together with comparative data for the known $[Me_3TACN]Y(CH_2SiMe_3)_3$ (**8**)[18] precursor. Addition of 1 equiv of activator per molecule of **2a′** (Y:act = 2:1) results in single-site catalyst behavior, whereas addition of 2 equiv of activator (Y:act = 2:2) results in a higher activity, but also in a broad molecular weight distribution (M_w/M_n = 7.7). In fact, the result from this experiment is close to that of **2a** with anilinium borate activator at the same temperature. It can be seen from Table 9 that reaction of **8** with either 1 or 2 equiv of activator results in single-site behavior. As it is likely that the reaction of **2a′** with the first batch of activator results initially in the abstraction of an alkyl group from the Y-trialkyl moiety, it seems that the involvement of multiple active species due to partial ligand scrambling in the **2a** catalyst system is a realistic possibility. Why this would be particularly prominent in the Y catalysts with a *t*BuN moiety is presently unclear.

Conclusions

The synthesis of a series of rare earth metal dialkyl complexes with *N*,*N*′-dimethyl−TACN−amide ancillary ligands has allowed the comparative testing of their cationic monoalkyl derivatives in the catalytic polymerization of ethylene. The effect on catalyst performance of variation in the ionic radius of the trivalent metal center (a unique feature for rare earth metal catalysts) appears to be substantially larger than that of variation in ligand substitution pattern or ligand geometric constraint. Nevertheless, these ligand features may be used to fine-tune catalyst performance, in this case the molecular weight of the produced polyethylene or the thermal stability of the catalyst. Cationic rare earth metal alkyl catalysts thus have a wide range of variables that can be used to tune reactivity. It is expected that an increased understanding of ligand structure−catalyst property relationships for cationic rare earth metal alkyl catalysts will allow them to be used with a wider scope.

Experimental Section

General Remarks. All preparations were performed under an inert nitrogen atmosphere, using standard Schlenk or glovebox techniques, unless stated otherwise. Toluene, pentane, and hexane (Aldrich, anhydrous, 99.8%) were passed over columns of Al_2O_3 (Fluka), BASF R3-11-supported Cu oxygen scavenger, and molecular sieves (Aldrich, 4 Å). Diethyl ether and THF (Aldrich, anhydrous, 99.8%) were dried over Al_2O_3 (Fluka). All solvents were degassed prior to use and stored under nitrogen. Deuterated solvents (C_6D_6, C_7D_8, C_4D_8O; Aldrich) were vacuum transferred from Na/K alloy prior to use. Reagents: Me_3SiCH_2Li,[19] $YCl_3(THF)_{3.5}$, $LaBr_3(THF)_4$,[20] $Y(CH_2SiMe_3)_3(THF)_2$.[21] The ligands **L1**$^{a-c}$ and **L2**^{a,b} were prepared analogously to the related ligands with the *i*Pr_2TACN fragment.[5d] Full description of their synthesis and characterization is given in the Supporting Information. $[PhNMe_2H][B(C_6F_5)_4]$ and $[Ph_3C][B(C_6F_5)_4]$ (Strem) were used as received. NMR spectra were recorded on Varian Gemini VXR 300 or Varian Inova 500 spectrometers in NMR tubes equipped with a Teflon (Young) valve. The ^{1}H NMR spectra were referenced to resonances of residual protons in deuterated solvents. The ^{13}C NMR spectra were referenced to carbon resonances of deuterated solvents and reported in ppm relative to TMS (δ 0 ppm). Ethylene (AGA polymer grade) was passed over columns with supported copper scavenger (BASF R3-11) and molecular sieves (4 Å) before being passed to the reactor. GPC analyses were performed by A. Jekel on a Polymer Laboratories Ltd. (PL-GPC210) chromatograph using 1,2,4-trichlorobenzene (TCB) as the mobile phase at 150 °C and using polystyrene references.

Synthesis of $[Me_2TACN(SiMe_2)N$*t*$Bu]Sc(CH_2SiMe_3)_2$ (1a). At ambient temperature, a solution of $Me_2TACN(SiMe_2)NH$*t*Bu (0.28 g, 1.00 mmol) in pentane (10 mL) was added dropwise to a solution of $Sc(CH_2SiMe_3)_3(THF)_2$ (0.45 g, 1.00 mmol) in pentane (50 mL). The reaction mixture was stirred overnight, after which the volatiles were removed in a vacuum. The residue was stripped of remaining THF by stirring with 5 mL of pentane, which was subsequently removed under reduced pressure. The resulting solid was extracted with pentane (2 × 50 mL) and concentrated. Cooling the extract to −30 °C produces the crystalline title compound (0.35 g, 0.70 mmol, 70%). Compound **1b** was prepared analogously.

^{1}H NMR (500 MHz, 25 °C, C_6D_6) δ: 2.92 (t, $^2J_{HH}$ = 5.9 Hz, 1 H, NCH_2), 2.89 (t, J_{HH} = 5.9 Hz, 1 H, NCH_2), 2.41 (m, 2 H, NCH_2), 2.37 (s, 6 H, NMe), 2.34−2.30 (m, 2 H, NCH_2), 1.90−1.85 (m, 2 H, NCH_2), 1.83−1.78 (m, 2 H, NCH_2), 1.76−1.72 (m, 2 H, NCH_2), 1.53 (s, 9 H, *t*Bu), 0.44 (s, 18 H, $CH_2Si\mathit{Me}_3$), 0.28 (s, 6 H, $Si\mathit{Me}_2$), −0.06 (d, J_{HH} = 10.5 Hz, 2 H, Sc*CH*H), −0.38 (dd, J_{HH} = 10.5 Hz, 2 H, ScCH*H*). ^{13}C NMR (125.7 MHz, 25 °C, C_6D_6) δ: 58.5 (t, J_{CH} = 132.0 Hz, NCH_2), 56.5 (t, J_{CH} = 131.6 Hz, NCH_2), 52.9 (s, *t*Bu C), 51.2 (q, J_{CH} = 137.5 Hz, NMe), 46.8 (t, J_{CH} = 134.5 Hz, NCH_2), 36.9 (q, J_{CH} = 122.9 Hz, *t*Bu Me), 36.2 ($ScCH_2$), 5.1

(17) Bambirra, S.; van Leusen, D.; Meetsma, A.; Hessen, B.; Teuben, J. H. *Chem. Commun.* **2003**, 522.

(18) Lawrence, S. C.; Ward, B. D.; Dubberley, S. R.; Kozak, C. M.; Mountford P. *Chem. Commun.* **2003**, 2880.

(19) Lewis, H. L.; Brown, T. L. *J. Am. Chem. Soc.* **1970**, *92*, 4664.

(20) $LaBr_3$: Taylor, M. D.; Carter, C. P. *J. Inorg. Nucl. Chem.* **1962**, *24*, 387. $LaBr_3(THF)_4$: Herzog, S.; Gustav, K.; Krüger, E.; Oberender, H.; Schuster, R. *Z. Chem.* **1963**, *3*, 428.

(21) Lappert, M. F.; Pearce, R. *J. Chem. Soc., Chem. Commun.* **1973**, 126.

Table 10. Crystal Data and Collection Parameters of Complexes 2a′, 3a, 3b, 5a, 6a, and 7b

	2a′	3a	3b	5a	6a	7b
formula	$C_{44}H_{106}N_8Si_4Y_2$-$(C_7H_8)_{0.5}$	$C_{22}H_{55}N_4Si_3Y$	$C_{22}H_{55}N_4Si_3Y$	$C_{22}H_{53}N_4Si_2Nd$	$C_{22}H_{55}N_4Si_3Nd$	$C_{18}H_{44}N_4Si_2ScCl$
fw	1083.60	548.88	548.88	574.10	604.20	453.15
cryst color	colorless	colorless	colorless	sky blue	sky blue	colorless
cryst size, mm	0.32 × 0.18 × 0.13	0.51 × 0.22 × 0.06	0.41 × 0.22 × 0.11	0.12 × 0.20 × 0.50	0.10 × 0.09 × 0.08	0.15 × 0.12 × 0.08
cryst syst	orthorhombic	orthorhombic	monoclinic	monoclinic	orthorhombic	orthorhombic
space group	*Fdd*2, 43	$P2_12_12_1$, 19	$P2_1/c$, 14	$P2_1/n$, 14	$P2_12_12_1$, 19	*Pbca*, 61
a, Å	34.635(1)	10.5666(6)	10.3025(6)	8.5802(4)	10.682(7)	16.804(1)
b, Å	36.689(1)	11.4796(7)	11.8052(7)	17.5788(8)	11.598(8)	15.941(1)
c, Å	19.5786(6)	26.277(2)	26.510(1)	19.7663(9)	26.59(2)	19.455(2)
α,deg	90.00(1)	90.00(1)	90.00(1)	90.00(1)	90.00(1)	90.00(1)
β, deg	90.00(1)	90.00(1)	97.24(1)	99.552(1)	90.00(1)	90.00(1)
γ, deg	90.00(1)	90.00(1)	90.00(1)	90.00(1)	90.00(1)	90.00(1)
V, Å^3	24879.0(12)	3187.4(4)	3198.5(3)	2940.0(2)	3294(4)	5211.5(7)
Z	16	4	4	4	4	8
ρ_{calcd}, g cm^{-3}	1.157	1.144	1.140	1.297	1.218	1.155
μ, cm^{-1}	19.69	19.57	19.5	18.62	16.99	4.87
R1	0.0519	0.0432	0.0467	0.0203	0.0471	0.0495
wR2 (all data)	0.1224	0.1098	0.1308	0.0425	0.1063	0.1292
largest e_{max}, e_{min}, e Å^{-3}	0.75(9), −0.96	0.51(6), −0.41	0.49(6), −0.29	0.95(7), −0.35	0.70(9), −0.58	0.67(6), −0.63
temp, K	110(1)	230	230	90(1)	230(1)	230(2)
GOF	1.034	1.004	1.009	0.912	1.036	1.009

(q, J_{CH} = 116.4 Hz, $CH_2Si\mathit{Me}_3$), 4.4 (q, J_{CH} = 117.6 Hz, $Si\mathit{Me}_2$). Anal. Calcd for $C_{22}H_{55}N_4Si_3Sc$: C, 52.33; H, 10.98; N, 11.10. Found: C, 51.90; H, 10.65; N, 10.88.

Synthesis of [Me$_2$TACN(CH$_2$)$_2$N*t*Bu]Y(CH$_2$SiMe$_3$)$_2$ (2a). A solution of $Me_2TACN(CH_2)_2NH\mathit{t}Bu$ (0.25 g, 1.00 mmol) in THF (10 mL) was added dropwise to a solution of $Y(CH_2SiMe_3)_3(THF)_2$ (0.49 g, 1.00 mmol) in THF (30 mL) at ambient temperature. The reaction mixture was stirred for 3 h, after which the volatiles were removed in vacuo. The residue was stripped of residual THF by stirring with pentane (5 mL), which was subsequently removed in vacuo. The resulting solid was extracted with pentane (2 × 100 mL). Concentrating and cooling the extract to −30 °C gives the title compound as a crystalline solid (0.41 g, 0.80 mmol, 80%). Compound **2b** was prepared analogously.

^{1}H NMR (500 MHz, −60 °C, C_7D_8) δ: 3.32 (m, 1 H, NCH_2), 3.12−3.00 (m, 2 H, NCH_2), 2.87−2.69 (m, 3H, NCH_2), 2.33 (m, 1 H, NCH_2), 2.33 (s, 3 H, NMe), 2.22 (m, 1 H, NCH_2), 2.16 (s, 3 H, NMe_2), 1.76−1.56 (m, 4H, NCH_2), 1.52 (s, 9 H, *t*Bu), 1.39 (m, 4 H, NCH_2), 0.64 (s, 9 H, Me_3SiCH_2), 0.57 (s, 9 H, Me_3SiCH_2), −0.62 (d, J_{HH} = 11.0 Hz, 1 H, Me_3SiCH_2), −0.86 (d, J_{HH} = 11.0 Hz, 1 H, Me_3SiCH_2), −0.94 (d, J_{HH} = 10.5 Hz, 1 H, Me_3SiCH_2), −1.06 (d, J_{HH} = 10.5 Hz, 1 H, Me_3SiCH_2). The J_{YH} coupling on the YCH_2 protons is unresolved. ^{13}C NMR (125.7 MHz, −60 °C, C_7D_8) δ: 59.8 (t, J_{CH} = 138.9 Hz, NCH_2), 58.9 (t, J_{CH} = 135.2 Hz, NCH_2), 57.5 (t, J_{CH} = 135.4 Hz, NCH_2), 54.8 (t, J_{CH} = 135.3 Hz, NCH_2), 53.9 (s, *t*Bu C), 53.1 (t, J_{CH} = 129.6 Hz, NCH_2), 51.4 (t, J_{CH} = 138.6 Hz, NCH_2), 49.3 (q, part. overlap, NMe), 48.9 (q, part. overlap, NMe), 48.4 (t, J_{CH} = 140.4 Hz, NCH_2), 47.0 (t, J_{CH} = 123.7 Hz, NCH_2), 30.8 (q, J_{CH} = 123.3, *t*Bu Me), 29.8 (dt, J_{YC} = 35.4 Hz, J_{CH} = 93.3 Hz, YCH_2), 28.5 (dt, J_{YC} = 38.9 Hz, J_{CH} = 97.3 Hz. YCH_2), 5.2 (q, J_{CH} = 116.9 Hz, Me_3SiCH_2Y), 5.1 (q, J_{CH} = 116.5 Hz, Me_3SiCH_2Y). Anal. Calcd for $C_{22}H_{53}N_4Si_2Y$: C, 50.94; H, 10.30; N, 10.80. Found: C, 51.0; H, 10.27; N, 10.65.

Reaction of [Me$_2$TACN(CH$_2$)$_2$N*t*Bu)]Y(CH$_2$SiMe$_3$)$_2$ (2a) with [HNMe$_2$Ph][B(C$_6$F$_5$)$_4$]. A solution of **2a** (20 mg, 38.5 μmol) in C_6D_5Br (0.6 mL) was added to $[HNMe_2Ph][B(C_6F_5)_4]$ (30 mg, 38.5 μmol). The obtained solution was transferred to a NMR tube and analyzed by NMR spectroscopy, which showed full conversion to the corresponding cationic monoalkyl species, $SiMe_4$, and free $PhNMe_2$.

^{1}H NMR (500 MHz, 20 °C, C_6D_5Br) δ: 2.66 (m, 4 H, NCH_2), 2.54 (m, 4 H, NCH_2), 2.36 (m, 8 H, NCH_2) 2.26 (s, 6 H, TACN $N\mathit{Me}$), 1.11 (s, 9 H, *t*Bu), 0.08 (s, 9 H, $CH_2Si\mathit{Me}_3$), −1.01 (d, $^1J_{YH}$ = 2.82 Hz, 2 H, $C\mathit{H}_2SiMe_3$). ^{13}C{^{1}H} NMR (125.7 MHz, C_6D_5Br, 20 °C) δ: 60.1 (NCH_2), 56.1 (NCH_2), 54.2 (*t*Bu C), 53.7 (NCH_2), 51.8 (NCH_2), 46.5 (TACN $N\mathit{Me}$), 46.2 (NCH_2), 37.0 (d, J_{YC} = 40.7 Hz, $Y\mathit{C}H_2$), 30.2 (*t*Bu Me), 4.0 ($YCH_2Si\mathit{Me}_3$). ^{19}F NMR (470 MHz, 20 °C, C_6D_5Br) δ: −137.17 (d, J_{FF} = 10.3 Hz, *o*-CF), −167.23 (d, J_{FF} = 20.7 Hz, *p*-CF), −171.22 (d, J_{FF} = 16.9 Hz, *m*-CF).

Reaction of [Me$_2$TACN(CH$_2$)$_2$N*t*Bu)]Y(CH$_2$SiMe$_3$)$_2$ (2a) with [Ph$_3$C][B(C$_6$F$_5$)$_4$]. A solution of **2a** (26 mg, 50.0 μmol) in C_6D_5Br (0.6 mL) was added to $[Ph_3C][B(C_6F_5)_4]$ (46 mg, 50.3 μmol). The obtained solution was transferred to an NMR tube and analyzed by NMR spectroscopy, which showed conversion to the corresponding cationic monoalkyl species and $Ph_3CCH_2SiMe_3$.[22] ^{1}H NMR (500 MHz, 20 °C, C_6D_5Br) δ: 2.64 (m, 4 H, NCH_2), 2.52 (m, 4 H, NCH_2), 2.36 (m, 8 H, NCH_2) 2.24 (s, 6 H, TACN $N\mathit{Me}$), 1.10 (s, 9 H, *t*Bu), 0.05 (s, 9 H, $CH_2Si\mathit{Me}_3$), −1.03 (d, J_{YH} = 2.8 Hz, 2 H, $C\mathit{H}_2SiMe_3$). ^{13}C{^{1}H} NMR (125.7 MHz, C_6D_5Br, 20 °C) δ: 60.1 (NCH_2), 56.0 (NCH_2), 54.2 (*t*Bu C), 53.8 (NCH_2), 51.9 (NCH_2), 46.5 (TACN $N\mathit{Me}$), 46.4 (NCH_2), 37.3 (d, J_{YC} = 40.2 Hz, $Y\mathit{C}H_2$), 30.2 (*t*Bu Me), 4.0 ($YCH_2Si\mathit{Me}_3$). $Ph_3CCH_2SiMe_3$: ^{13}C-{^{1}H} NMR (125.7 MHz, C_6D_5Br, 20 °C) δ: 149.0, 143.9 (ipso-C $Ph_3CCH_2SiMe_3$), 129.4, 129.0 ($\mathit{Ph}_3CCH_2SiMe_3$), 128.3, 127.6 (Ph_3-CCH_2SiMe_3), 126.2, 125.7 ($\mathit{Ph}_3CCH_2SiMe_3$), 31.7, 26.3 ($Ph_3C\mathit{C}H_2$-$SiMe_3$), 0.5, −1.9 ($Ph_3CCH_2Si\mathit{Me}_3$).

Synthesis of [Me$_2$TACN(CH$_2$)$_2$N*n*Bu]Y(CH$_2$SiMe$_3$)$_2$ (2c). A solution of $Me_2TACN(CH_2)_2NH\mathit{n}Bu$ (0.76 g, 2.96mmol) in pentane (10 mL) was added dropwise to a solution of $(Me_3SiCH_2)_3Y(THF)_2$ (1.46 g, 2.96 mmol) in pentane (50 mL) at ambient temperature. The reaction mixture was stirred overnight, after which the volatiles were removed in vacuum. The residue was stripped of residual THF by stirring with pentane (5 mL), which was subsequently removed in vacuum. The resulting sticky solid was extracted with pentane (4 × 20 mL). Concentrating and cooling the extract to −30 °C gives the product as a crystalline solid (1.08 g, 2.10 mmol, 71%).

^{1}H NMR (500 MHz, 25 °C, C_7D_8) δ: 3.29 (t, J_{HH} = 7.5 Hz, 2 H, $C\mathit{H}_2CH_2CH_2Me$), 3.04 (m, 2 H, NCH_2), 2.26 (s, 6 H, NMe), 2.08 (m, 8 H, NCH_2), 1.74 (m, 6 H, NCH_2), 1.57 (m, 2 H, $CH_2C\mathit{H}_2$-CH_2Me), 1.54 (m, 2 H, $CH_2CH_2C\mathit{H}_2Me$), 1.09 (t, J_{HH} = 7.0 Hz, 3 H, $CH_2CH_2CH_2\mathit{Me}$), 0.40 (s, 18 H, $CH_2Si\mathit{Me}_3$), −0.79 (d, J_{HH} = 10.5 Hz, 2 H, $C\mathit{H}_2SiMe_3$), −0.94 (d, J_{HH} = 10.5 Hz, 2 H, $C\mathit{H}_2$-$SiMe_3$). ^{13}C NMR (125.7 MHz, 25 °C, C_7D_8) δ: 60.4 (t, J_{CH} = 138.4, $N\mathit{C}H_2CH_2CH_2Me$), 54.7 (t, J_{CH} = 128.5 Hz, NCH_2), 54.6

(22) Bolton, P. D.; Clot, E.; Adams, N.; Dubberley, S. R.; Cowley, A. R.; Mountford, P. *Organometallics* **2006**, *25*, 2806.

(t, J_{CH} = 128.5 Hz, NCH_2) (all other NCH_2 resonances obscured due to broadening), 48.8 (q, J_{CH} = 136.4 Hz, N*Me*), 34.5 (t, J_{CH} = 124.4 Hz, $NCH_2CH_2CH_2Me$), 29.3 (dt, J_{YC} = 35.9 Hz, J_{CH} = 98.2 Hz, YCH_2SiMe_3), 21.8 (t, J_{CH} = 124.1 Hz, $NCH_2CH_2CH_2Me$), 14.8 (q, J_{CH} = 124.7 Hz, $NCH_2CH_2CH_2Me$), 5.0 (q, J_{CH} = 115.9 Hz, CH_2SiMe_3). ^{13}C NMR (125.7 MHz, −40 °C, C_7D_8) δ: 60.1 (t, J_{CH} = 134.1 Hz, $NCH_2CH_2CH_2Me$), 59.0 (t, J_{CH} = 138.4 Hz, NCH_2), 57.0 (t, J_{CH} = 132.0 Hz, NCH_2), 54.8 (t, J_{CH} = 127.6 Hz, NCH_2), 54.7 (t, J_{CH} = 128.1 Hz, NCH_2), 54.4 (t, J_{CH} = 136.3 Hz, NCH_2), 52.9 (t, J_{CH} = 132.0 Hz, NCH_2), 51.1 (t, J_{CH} = 132.2 Hz, NCH_2), 49.4 (t, J_{CH} = 134.1 Hz, NCH_2), 48.6 (q, J_{CH} = 136.3 Hz, N*Me*), 34.7 (t, J_{CH} = 126.1 Hz, $NCH_2CH_2CH_2Me$), 29.6 (dt, J_{YC} = 36.5 Hz, J_{CH} = 97.2 Hz, YCH_2SiMe_3), 27.5 (dt, J_{YH} = 37.5 Hz, J_{CH} = 99.5 Hz, YCH_2SiMe_3), 22.0 (t, J_{CH} = 125.6 Hz, $NCH_2CH_2CH_2Me$), 15.3 (q, J_{CH} = 123.0 Hz, $NCH_2CH_2CH_2Me$), 5.4 (q, J_{CH} = 117.0 Hz, CH_2SiMe_3), 5.2 (q, J_{CH} = 117.0 Hz, CH_2SiMe_3). Anal. Calcd for $C_{22}H_{53}N_4Si_2Y$: C, 50.94; H, 10.30; N, 10.80; Y, 17.14. Found: C, 50.91; H, 10.33; N, 10.80; Y, 17.08.

[Me$_2$TACN(CH$_2$)$_2$N*n*Bu]Y(CH$_2$SiMe$_3$)$_2$ (2c) with [HNMe$_2$Ph][B(C$_6$F$_5$)$_4$]. A solution of **2c** (10.3 mg, 20 μmol) in C_6D_5Br (0.6 mL) was added to $[HNMe_2Ph][B(C_6F_5)_4]$ (18 mg, 20 μmol). The obtained solution was transferred to an NMR tube and analyzed by NMR spectroscopy, which showed full conversion to the corresponding cationic monoalkyl species, $SiMe_4$, and free $PhNMe_2$.

^{1}H NMR (500 MHz, 25 °C, C_6D_5Br) δ: (t, J = 7.2 Hz, 2 H, *m*-H $PhNMe_2$), 6.94 (t, J = 7.2 Hz, 1 H, *p*-H $PhNMe_2$), 6.38 (d, J = 7.2 Hz, 2 H, *o*-H $PhNMe_2$), 3.98 (t, J = 7.0 Hz, 2 H, $CH_2CH_2CH_2Me$), 2.72 (m, 2 H, NCH_2), 2.68 (s, 6 H, NMe), 2.51 (m, 4 H, NCH_2), 2.36−2.18 (m, 10 H, NCH_2), 1.31 (m, 2 H, $CH_2CH_2CH_2Me$), 0.97 (t, J = 7.0 Hz, 3 H, $CH_2CH_2CH_2Me$), 0.88 (m, 2 H, $CH_2CH_2CH_2Me$), 0.08 (s, 9 H, CH_2SiMe_3), −1.10 (2 H, CH_2SiMe_3). ^{13}C NMR (125.7 MHz, 25 °C, C_6D_5Br) δ: 60.9 (t, J_{CH} = 138.4, $NCH_2CH_2CH_2Me$), 52.5 (t, J_{CH} = 128.5 Hz, NCH_2), 50.3 (NMe) (all other NCH_2 resonances obscured due to broadening), 33.6 ($NCH_2CH_2CH_2Me$), 31.8 (dt, J_{YC} = 46.4 Hz, YCH_2SiMe_3), 20.9 ($NCH_2CH_2CH_2Me$), 14.3 ($NCH_2CH_2CH_2Me$), 3.9 (q, J_{CH} = 116.9 Hz, CH_2SiMe_3).

Synthesis of {[η^3:η^1-[Me$_2$TACN(CH$_2$)$_2$NtBu]Y(CH$_2$SiMe$_3$)}-{η^3:μ-η^1-[Me$_2$TACN(CH$_2$)$_2$N*t*Bu]Y(CH$_2$SiMe$_3$)$_3$} (2a′). A solution of Me$_2$TACN-(CH$_2$)$_2$NH*t*Bu (0.25 g, 1.00 mmol) in pentane (5 mL) was added dropwise to a solution of $Y(CH_2SiMe_3)_3(THF)_2$ (0.49 g, 1.00 mmol) in pentane (50 mL) at ambient temperature. The reaction mixture was stirred for 2 h, during which time a white precipitate had formed. The volatiles were removed in a vacuum, and the residue was analyzed by ^{1}H NMR (C_6D_6). The spectrum displays the resonances of **2a** and the title compound in a 1:1 ratio. The crude mixture was extracted with pentane (2 × 40 mL), leaving pure dimer **2a′** as a white powder (0.19 g, 36% calculated on Y).

^{1}H NMR (500 MHz, 20 °C, C_6D_6) δ: 4.19 (m, 1 H, NCH_2), 3.31 (m, 1 H, NCH_2), 3.23 (t, J_{HH} = 11.5 Hz, 2 H, NCH_2), 3.12−2.90 (m, 7H, NCH_2), 2.75−2.64 (m, 4 H, NCH_2), 2.51 (s, 3 H, NMe), 2.41 (s, 6 H, NMe), 2.38 (s, 3 H, NMe), 2.28−2.23 (m, 3 H, NCH_2), 2.15−2.05 (m, 6 H, NCH_2), 1.92−1.75 (m, 6 H, NCH_2), 1.58 (s, 9 H, *t*Bu), 1.55 (m, 2 H, NCH_2), 1.47 (s, 9 H, *t*Bu), 0.52 (s, 9 H, Me_3SiCH_2), 0.50 (s, 9 H, Me_3SiCH_2), 0.43 (s, 9 H, Me_3SiCH_2), 0.40 (s, 9 H, Me_3SiCH_2), −0.40 (d, J_{HH} = 10.6 Hz, J_{YH} = 2.5 Hz, 2 H, Me_3SiCH_2), −0.62 (d, J_{HH} = 11.0 Hz, J_{YH} = 2.5 Hz 2 H, Me_3SiCH_2), −0.78 (d, J_{HH} = 10.5 Hz, 4 H, Me_3SiCH_2). The J_{YH} coupling on the YCH_2 protons is unresolved. ^{13}C{H} NMR (125.7 MHz, 20 °C, C_6D_6) δ: 61.6 (NCH_2), 59.1 (NCH_2), 57.4 (NCH_2), 56.1 (s, *t*Bu C), 55.6 (NCH_2), 55.1 (NCH_2), 54.3 (NCH_2), 54.1 (NCH_2), 53.8 (NCH_2), 53.3 (s, *t*Bu C), 52.8 (NCH_2), 51.4 (NCH_2), 51.1 (NCH_2), 50.7 (NCH_2), 49.3 (NCH_2), 49.0 (NCH_2), 48.2, 48.1, 48.0 (NMe), 42.7 (NCH_2), 39.6 (dt, J_{YC} = 33.0 Hz, YCH_2), 34.4 (*t*Bu Me), 34.0 (dt, J_{YC} = 34.7 Hz, YCH_2), 33.7 (dt, J_{YC} = 34.5 Hz, YCH_2), 31.2 (*t*Bu Me), 5.5, 5.4, 5.2, 4.9 (Me_3SiCH_2). Anal. Calcd for $C_{44}H_{106}N_8Si_4Y_2$: C, 50.94; H, 10.30; N, 10.80. Found: C, 50.60; H, 10.22; N, 10.34.

Synthesis of [Me$_2$TACN(SiMe$_2$)N*t*Bu]Y(CH$_2$SiMe$_3$)$_2$ (3a). At ambient temperature, a solution of Me$_2$TACN(SiMe$_2$)NH*t*Bu (0.65 g, 2.28 mmol) in pentane (10 mL) was added dropwise to a solution of $Y(CH_2SiMe_3)_3(THF)_2$ (1.12 g, 2.28 mmol) in pentane (60 mL). The reaction mixture was stirred for 2 h, after which the volatiles were removed in vacuo. The residue was stripped of remaining THF by stirring with 5 mL of pentane, which was subsequently removed under reduced pressure. The resulting sticky solid was then extracted with pentane (2 × 60 mL) and concentrated. Cooling the extract to − 30 °C produces the crystalline title compound (0.92 g, 1.67 mmol, 73%). Compound **3b** was prepared analogously.

^{1}H NMR (300 MHz, 25 °C, C_6D_6) δ: 2.85−2.76 (m, 2 H, NCH_2), 2.30 (s, 6 H, NMe), 2.25−2.11 (m, 4 H, NCH_2), 1.88−1.62 (m, 6 H, NCH_2), 1.51 (s, 9 H, *t*Bu), 0.45 (s, 18 H, CH_2SiMe_3), 0.26 (s, 6 H, $SiMe_2$), −0.51 (dd, J_{HH} = 10.5 Hz, J_{YH} = 3.0 Hz, 2 H, YC*H*H), −0.76 (dd, J_{HH} = 10.5 Hz, J_{YH} = 3.0 Hz, 2 H, YCH*H*). ^{13}C NMR (500 MHz, 25 °C, C_6D_6) δ: 57.2 (t, J_{CH} = 132.1 Hz, NCH_2), 55.1 (t, J_{CH} = 128.9 Hz, NCH_2), 52.5 (s, *t*Bu C), 50.0 (q, J_{CH} = 134.0 Hz, NMe), 45.9 (t, J_{CH} = 133.7 Hz, NCH_2), 36.6 (q, J_{CH} = 124.0 Hz, *t*Bu Me), 32.9 (dt, J_{CH} = 96.6 Hz, J_{YH} = 37.0 Hz, YCH_2), 5.2 (q, J_{CH} = 116.0 Hz, CH_2SiMe_3), 4.1 (q, J_{CH} = 116.0 Hz, $SiMe_2$). Anal. Calcd for $C_{22}H_{55}N_4Si_3Y$: C, 48.14; H, 10.10; N, 10.21; Y, 16.20. Found: C, 47.93; H, 10.95; N, 10.25; Y, 16.19.

Reaction of [Me$_2$TACN(SiMe$_2$)N*t*Bu)]Y(CH$_2$SiMe$_3$)$_2$ (3a) with [HNMe$_2$Ph][B(C$_6$F$_5$)$_4$]. A solution of **3a** (27 mg, 49.3 μmol) in C_6D_5Br (0.6 mL) was added to $[HNMe_2Ph][B(C_6F_5)_4]$ (39 mg, 49.3 μmol). The obtained solution was transferred to an NMR tube and analyzed by NMR spectroscopy, which showed full conversion to the corresponding cationic monoalkyl species, $SiMe_4$, and free $PhNMe_2$. ^{1}H NMR (500 MHz, −30 °C, C_6D_5Br) δ: 2.70−2.67 (m, 2 H, NCH_2), 2.46−2.44 (m, 2 H, NCH_2), 2.35−2.25 (m, 8 H, NCH_2), 2.14 (s, 6 H, TACN N*Me*), 1.18 (s, 9 H, *t*Bu), 0.04 (s, 9 H, CH_2SiMe_3), 0.03 (s, 6 H, $SiMe_2$), −0.89 (br, 2 H, CH_2SiMe_3). ^{13}C NMR (125.7 MHz, −30 °C, C_6D_5Br) δ: 56.4 (t, J_{CH} = 135.4 Hz, NCH_2), 53.3 (s, *t*Bu C), 52.9 (t, J_{CH} = 140.2 Hz, NCH_2), 46.4 (q, J_{CH} = 137.0 Hz, TACN N*Me*), 45.5 (t, J_{CH} = 138.6 Hz, NCH_2), 40.1 (q, J_{CH} = 140.2 Hz, *t*Bu Me), 39.7 (dt, J_{CH} = 91.9 Hz, J_{YC} = 42.0 Hz, YCH_2), 3.9 (q, J_{CH} = 117.7 Hz, YCH_2SiMe_3), 2.7 (q, J_{CH} = 117.7 Hz, $SiMe_2$).

Synthesis of [Me$_2$TACN(CH$_2$)$_2$N*t*Bu]La(CH$_2$SiMe$_3$)$_2$ (4a). Solid $LiCH_2SiMe_3$ (0.28 g, 3.00 mmol) was added to a suspension of $LaBr_3(THF)_4$ (0.67 g, 1.00 mmol) in THF (60 mL, ambient temperature). Within 5 min a bright yellow solution was formed. The solution was stirred for 3 h, after which it was reacted with Me$_2$TACN(CH$_2$)$_2$NH*t*Bu (0.25 g, 1.00 mmol), and this solution was stirred for 3 h, after which the volatiles were removed in vacuo. The mixture was extracted with pentane (2 × 50 mL), and the obtained extract was concentrated to 20 mL and cooled (− 30 °C), yielding the product (0.25 g, 0.44 mmol, 48%).

^{1}H NMR (500 MHz, 25 °C, C_6D_6) δ: 3.08 (m, 2 H, NCH_2), 2.82 (m, 2 H, NCH_2), 2.40−2.35 (m, 2 H, NCH_2), 2.27 (s, 6 H, NMe_2), 2.17−2.13 (m, 4 H, NCH_2), 1.79−1.74 (m, 2 H, NCH_2), 1.71−1.66 (m, 3 H, NCH_2), 1.44 (s, 9 H, *t*Bu), 0.46 (s, 18 H, Me_3SiCH_2), −0.66 (d, J_{HH} = 10.5 Hz, 2 H, Me_3SiCH_2), −0.80 (d, J_{HH} = 10.5 Hz, 2 H, Me_3SiCH_2). ^{13}C NMR (125.7 MHz, 25 °C, C_6D_6) δ: 59.7 (t, J_{CH} = 131.6 Hz, NCH_2), 55.7 (t, J_{CH} = 135.0 Hz, NCH_2), 54.9 (s, *t*Bu C), 54.3 (t, J_{CH} = 133.4 Hz, NCH_2), 52.1 (t, J_{CH} = 129.8 Hz, NCH_2), 48.1 (t, J_{CH} = 103.6 Hz, $LaCH_2$), 47.5 (t, J_{CH} = 128.0 Hz, NCH_2), 47.0 (q, J_{CH} = 135.1 Hz, NMe), 30.2 (q, J_{CH} = 122.8, *t*Bu Me), 5.2 (q, J_{CH} = 115.8 Hz, Me_3SiCH_2). ^{1}H NMR (300 MHz, 20 °C, THF-d_8) δ: 3.14 (m, 2 H, NCH_2), 3.05 (m, 2H, NCH_2), 2.97−2.84 (m, 12 H, NCH_2), 2.68 (s, 6 H, NMe_2), 1.29 (s, 9 H, *t*Bu), −0.07 (s, 18 H, Me_3SiCH_2), −0.98 (d, J_{HH} = 8.0 Hz, 2 H, Me_3SiCH_2), −1.12 (d, J_{HH} = 8.0 Hz, 2 H, Me_3SiCH_2). ^{13}C NMR

(75.4 MHz, 20 °C, THF-d_8) δ: 61.5 (t, J_{CH} = 135.2 Hz, NCH_2), 57.8 (t, J_{CH} = 140.6 Hz, NCH_2), 56.5 (t, J_{CH} = 137.9 Hz, NCH_2), 56.3 (s, *t*Bu C), 54.1 (t, J_{CH} = 135.2 Hz, NCH_2), 49.1(t, J_{CH} = 127.1 Hz, NCH_2), 48.5 (q, J_{CH} = 135.2 Hz, NMe), 48.2 (t, J_{CH} = 102.8 Hz, $LaCH_2$), 31.4 (q, J_{CH} = 124.8, *t*Bu Me), 5.9 (q, J_{CH} = 116.9 Hz, Me_3SiCH_2). Anal. Calcd for $C_{22}H_{53}N_4LaSi_2$: C, 46.46; H, 9.39; N, 9.85. Found: C, 45.90; H, 9.21; N, 9.76.

Reaction of [Me_2TACN(CH_2)$_2$N*t*Bu)]La(CH_2SiMe_3)$_2$ (4a) with [$HNMe_2$Ph][$B(C_6F_5)_4$]. A solution of **4a** (11 mg, 20.0 μmol) in C_6D_5Br (0.6 mL) was added to [$HNMe_2$Ph][$B(C_6F_5)_4$] (16 mg, 20.0 μmol). The obtained solution was transferred to a NMR tube and analyzed by NMR spectroscopy, which showed full conversion to the cationic species {[Me_2TACN(CH_2)$_2$N*t*Bu]La(CH_2SiMe_3)(solv)$_n$}-[$B(C_6F_5)_4$], $SiMe_4$, and free $PhNMe_2$.

^{1}H NMR (500 MHz, −30 °C, C_6D_5Br) δ: 7.23 (t, J = 7.8 Hz, 2 H, *m*-H *Ph*NMe_2), 6.77 (t, J = 7.3 Hz, 1 H, *p*-H *Ph*NMe_2), 6.65 (d, J = 7.8 Hz, 2 H, *o*-H *Ph*NMe_2), 3.07 (br, 1 H, NCH_2), 2.93 (m, 2 H, NCH_2), 2.78 (br, 1 H, NCH_2), 2.66 (s, 6 H, PhN*Me*$_2$), 2.57−2.49 (m, 6 H, NCH_2), 2.41 (s, 3 H, TACN N*Me*), 2.29 (s, 3 H, TACN N*Me*), 2.17−2.06 (m, 6 H, NCH_2), 1.26 (s, 9 H, *t*Bu), 0.21 (s, 9 H, CH_2SiMe_3), 0.00 (s, 12 H, Si*Me*$_4$), −0.23 (br, 1 H, $LaCH_2$), −0.89 (d, $^2J_{HH}$ = 10.2 Hz, 1 H, $LaCH_2$).

Synthesis of [Me_2TACN(CH_2)$_2$N*t*Bu]Nd(CH_2SiMe_3)$_2$ (5a). Solid $LiCH_2SiMe_3$ (0.38 g, 3.30 mmol) was added to a suspension of $NdCl_3(THF)_3$ (0.51 g, 1.09 mmol) in THF (60 mL, ambient temperature). Within 5 min a bright blue solution was formed. The solution was stirred overnight, after which it was reacted with Me_2-TACN(CH_2)$_2$NH*t*Bu (0.25 g, 1.00 mmol). The resulting green solution was stirred for 3 h, after which the volatiles were removed in a vacuum. The mixture was extracted with pentane (2 × 50 mL), and the obtained green extract was concentrated to 20 mL and cooled (− 30 °C), yielding the product (0.26 g, 0.45 mmol 45%). Anal. Calcd for $C_{22}H_{53}N_4Si_2Nd$: C, 46.03; H, 9.31; N, 9.76; Nd, 25.12. Found: C, 45.58; H, 9.15; N, 9.75; Nd, 25.08. Compounds **5b**, **6a**, and **6b** were prepared analogously.

Synthesis of [Me_2TACN($SiMe_2$)N*t*Bu]ScCl(CH_2SiMe_3) (7a). At ambient temperature solid $LiCH_2SiMe_3$ (0.19 g, 2.00 mmol) was added to a suspension of $ScCl_3(THF)_3$ (0.36 g, 1.00 mmol) in THF (20 mL). The solution was stirred for 3 h, after which it was reacted with Me_2TACN($SiMe_2$)NH*t*Bu (0.28 g, 1.00 mmol). The reaction mixture was stirred overnight, after which the volatiles were removed in a vacuum. The residue was stripped of remaining THF by stirring with 5 mL of pentane, which was subsequently removed under reduced pressure. The residue was extracted with pentane (50 mL) and concentrated to 10 mL. Cooling the extract to −30 °C produces the crystalline title compound (0.29 g, 64%). Compound **7b** was prepared analogously.

^{1}H NMR (500 MHz, 25 °C, C_7D_8) δ: 3.16 (m, 1 H, NCH_2), 2.89 (m, 1 H, NCH_2), 2.55 (s, 3 H, NMe), 2.51−2.42 (m, 4 H, NCH_2), 2.40 (s, 3 H, NMe), 2.15−1.96 (m, 6 H, NCH_2), 1.48 (s, 9 H, *t*Bu), 0.45 (s, 9 H, CH_2SiMe_3), 0.38 (s, 3 H, Si*Me*$_2$), 0.24 (s, 3 H, Si*Me*$_2$), −0.01 (d, J_{HH} = 11.5 Hz, 1 H, ScC*H*H), −0.83 (d, J_{HH} = 11.5 Hz, 1 H, ScCH*H*). ^{13}C NMR (500 MHz, 25 °C, C_7D_8) δ: 59.5 (br t, J_{CH} = 138.07 Hz, NCH_2), 58.3 (br t, J_{CH} = 135.7 Hz, NCH_2), 57.1 (br t, J_{CH} = 134.24 Hz, NCH_2), 56.9 (br t, J_{CH} = 134.2 Hz, NCH_2), 52.9 (s, *t*Bu C), 51.3 (q, J_{CH} = 135.75 Hz, NMe), 50.9 (q, J_{CH} = 138.89 Hz, NMe), 47.4 (t, J_{CH} = 137.3 Hz, NCH_2), 47.1 (t, J_{CH} = 137.3 Hz, NCH_2), 36.4 (q, J_{CH} = 120.54 Hz, *t*Bu Me), 35.5 (br, Sc*C*H$_2$), 4.8 (q, J_{CH} = 117.4 Hz, CH_2SiMe_3), 3.7 (q, J_{CH} = 119.0 Hz, Si*Me*$_2$), 3.4 (q, J_{CH} = 119.0 Hz, Si*Me*$_2$). Anal. Calcd for $C_{18}H_{44}ClN_4ScSi_2$: C, 47.71; H, 9.79; N, 12.36. Found: C, 47.84; H, 9.82; N, 11.74.

Ethylene Polymerization Experiments. In a typical experiment, separate solutions of the appropriate [**L**M(CH_2SiMe_3)$_2$] compound (10 μmol) and of an equimolar amount of [$HNMe_2$Ph][$B(C_6F_5)_4$] or [Ph_3C][$B(C_6F_5)_4$] (10 μmol), each in 5 mL of toluene, were prepared in a glovebox. These were stored in separate serum-capped vials. Polymerization was performed in a stainless steel 0.5 L autoclave, predried and flushed with nitrogen, charged with 150 mL of dry toluene, equilibrated at the desired reaction temperature, and pressurized with ethylene (5 bar). The solution of [$HNMe_2$-Ph][$B(C_6F_5)_4$] or [Ph_3C][$B(C_6F_5)_4$] was injected into the reactor first (using a pneumatically operated injector), and the reaction was started by subsequently injecting the [**L**M(CH_2SiMe_3)$_2$] solution. The ethylene pressure was kept constant during the reaction by providing a replenishing flow. The reactor was stirred for the required reaction time and then vented. The polymer was repeatedly rinsed with methanol and dried in a vacuum oven. Experiments were carried out at 50 or 80 °C with run times of 10 min.

Acknowledgment. Financial support from ExxonMobil Chemicals and the National Research School Combination-Catalysis (NRSC-C) is gratefully acknowledged.

Supporting Information Available: Text giving full synthetic details and characterization for all compounds described in this paper (PDF); crystallographic data for **2a′**, **3a**, **3b**, **5a**, **6a**, and **7b** (CIF). This material is available free of charge via the Internet at http://pubs.acs.org.

OM060870A